



Redox-Hopping-Based Charge Transport Mediated by Ru(II)-Polypyridyl Species Immobilized in a Mesoporous Metal-Organic Framework

Jiaxin Duan, Subhadip Goswami and Joseph T. Hupp*

Department of Chemistry, Northwestern University, Evanston, IL, United States

OPEN ACCESS

Edited by:

Ali Reza Oveisi,
Zabol University, Iran

Reviewed by:

Zhaohui Li,
Fuzhou University, China
Junkuo Gao,
Zhejiang Sci-Tech University, China

*Correspondence:

Joseph T. Hupp
j-hupp@northwestern.edu

Specialty section:

This article was submitted to
Catalytic Engineering,
a section of the journal
Frontiers in Chemical Engineering

Received: 03 December 2021

Accepted: 23 December 2021

Published: 08 February 2022

Citation:

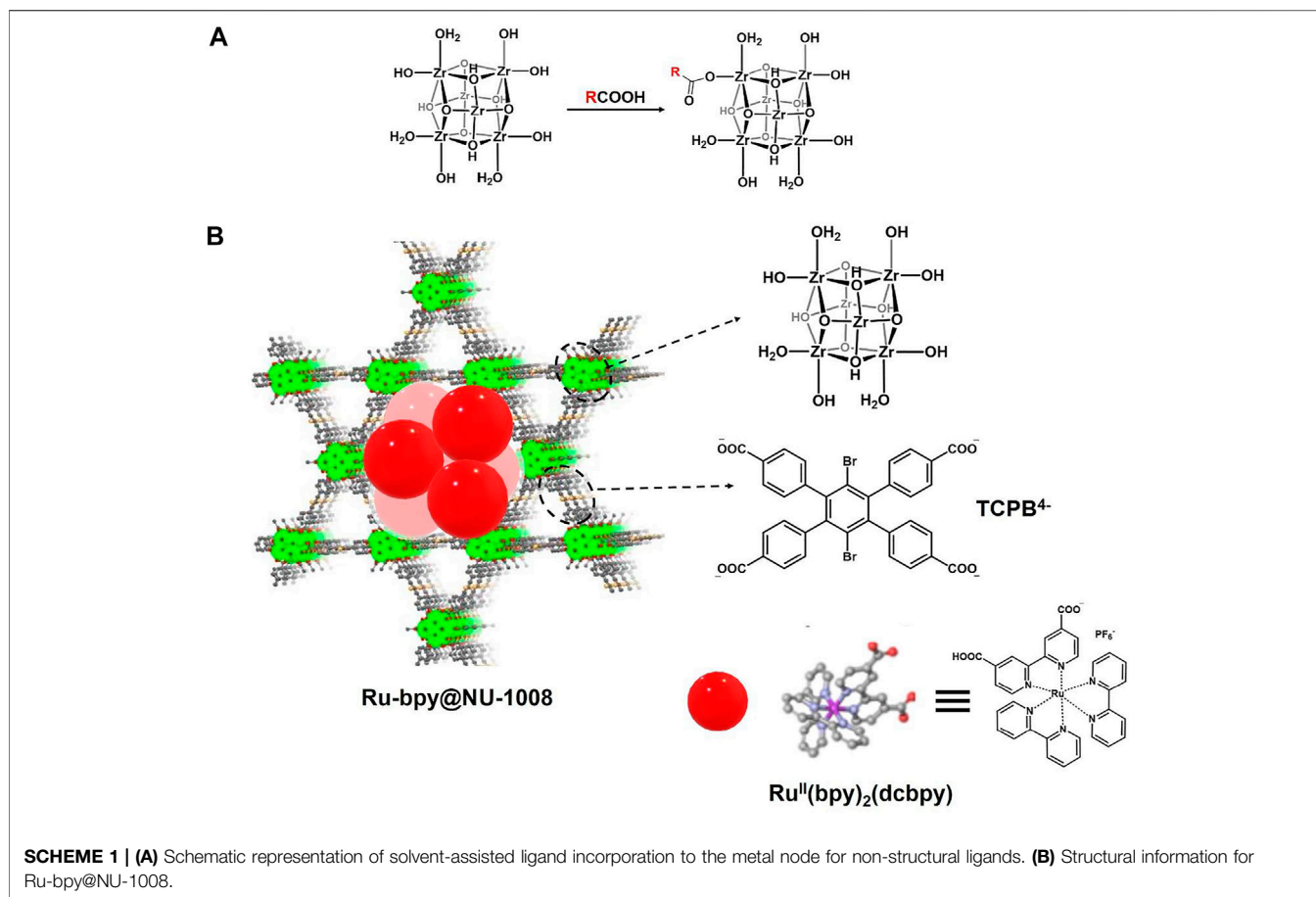
Duan J, Goswami S and Hupp JT
(2022) Redox-Hopping-Based Charge
Transport Mediated by Ru(II)-
Polypyridyl Species Immobilized in a
Mesoporous Metal-
Organic Framework.
Front. Chem. Eng. 3:828266.
doi: 10.3389/fceng.2021.828266

Electronic charge transport through crystalline metal-organic frameworks (MOFs) can be accomplished by site-to-site electron (or hole) hopping, provided that redox-active sites, such as easily reducible or oxidizable MOF linkers, are present. If the framework itself is redox-inert, solvent-assisted ligand incorporation of redox-active moieties can serve to enable hopping-based charge transport. Here we have studied the redox hopping process within Ru-bpy@NU-1008, where Ru-bpy is a carboxylate-functionalized derivative, *i.e.*, a node-ligating derivative, of the well-known chromophore Ru(2,2'-bipyridine)₃²⁺, and NU-1008 is a redox-inert MOF featuring hierarchical porosity and *csq* topology. Chronoamperometry experiments with electrode-supported thin films of Ru-bpy@NU-1008 show that charge transport is feasible through portions of the MOF, with other portions being inaccessible. Possible confounding features are the undersized *c*-pores that cross-connect 1D mesoporous channels, as ingress and egress of charge-compensating anions is believed to accompany the net oxidation of Ru(II) to Ru(III) and the reduction of Ru(III) to Ru(II). Phenomenologically, transport through the electroactive portion of the films is diffusion-like, with the magnitude of the apparent diffusion coefficient being $6 \times 10^{-12} \text{ cm}^2/\text{s}$.

Keywords: metal-organic framework (MOF), solvent-assisted linker incorporation (SALI), diffusion coefficient, redox hopping, charge transport

INTRODUCTION

The increasingly compelling demand for renewable, carbon-neutral sources of energy offers an incentive to develop catalytic materials that can seamlessly execute reactions analogous to those comprising naturally occurring photosynthesis, *e.g.*, water oxidation and chemical-energy-storing reduction of carbon dioxide. Compared to homogeneous catalysts, heterogeneous forms offer advantages in terms of (1) recyclability of the catalyst, (2) removing catalyst solubility as a design requirement, and (3) concentration and consolidation immediately proximal to an electrode or photoelectrode interface with a reactant-containing solution (Lieber and Lewis, 1984; Yoshida et al., 1993; Chen et al., 2009; Hod et al., 2015a). Metal-organic frameworks (MOFs), consisting of inorganic metal nodes and organic linkers, have shown promise as heterogeneous electro/photocatalysts (or catalyst supports) for solar fuel generation (Lei et al., 2018; Majewski et al., 2018; Johnson et al., 2020; Stanley et al., 2021). The broad synthetic tunability,

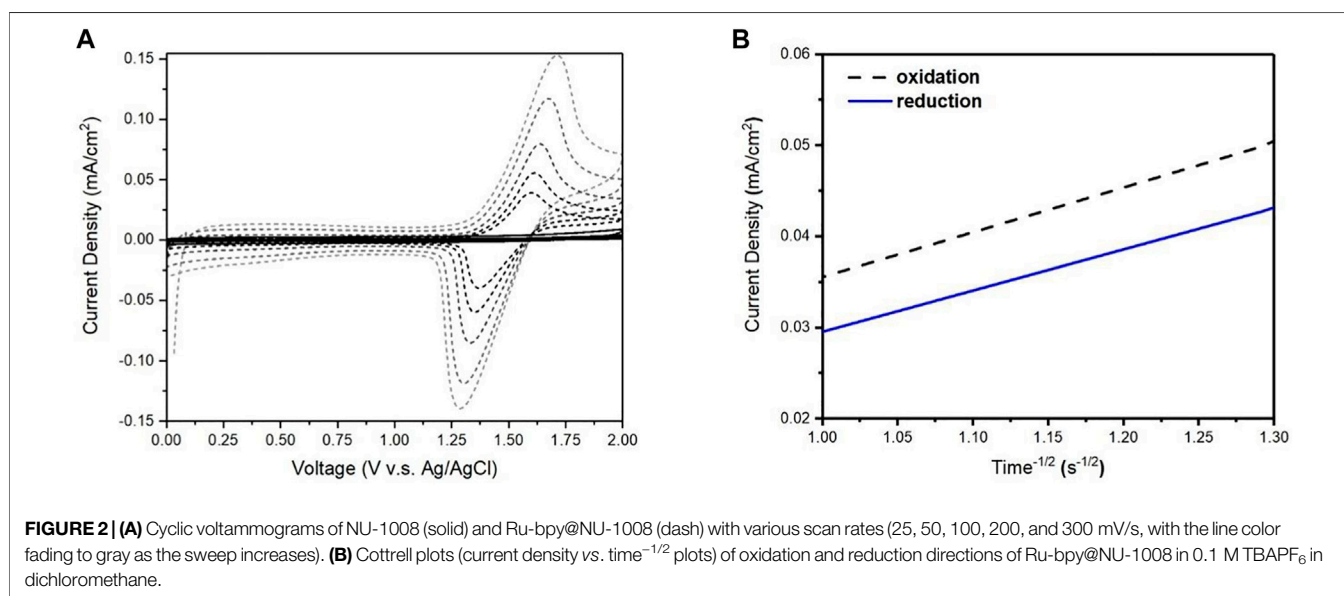
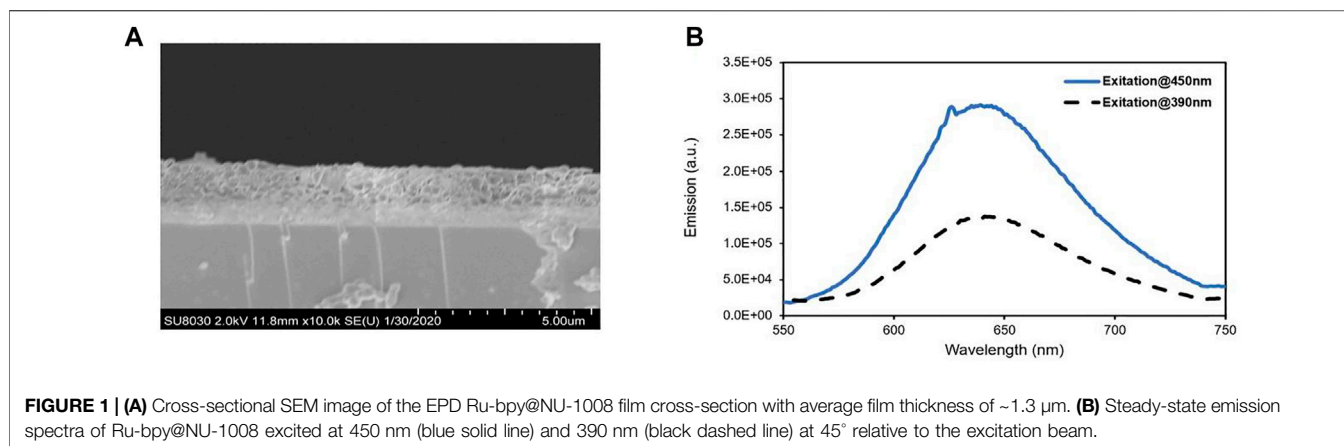


crystallographically well-defined periodic structures, and molecular-scale porosity of MOFs are among the features that make them attractive for these and other applications (Li et al., 2009; Furukawa et al., 2013; Islamoglu et al., 2017). Additionally, the fixed spatial separation of consecutive linker- or node-sited/grafted catalysts can delimit catalyst de-activation by dimerization or aggregation. MOFs can be made redox-active either by judiciously chosen redox-active organic linkers or redox-active metal nodes (Kung et al., 2020; Ding et al., 2021). Alternatively, they can be rendered redox-active by post-synthetic incorporation of redox-active species—for example, by chemically grafting and tethering to otherwise inactive nodes (Hod et al., 2015b; Celis-Salazar et al., 2019).

In MOF-based heterogeneous electrocatalysis, a crucial aspect, apart from the transport of substrate and electrolytes within the porous scaffold, is the transport of charges (Johnson et al., 2020). Due to the absence of any continuous pathway of charge movement in electronically localized MOFs, in electrode-supported MOF thin films, charges move from spatially separated linker to linker by redox hopping, a process that, on the macroscopic scale, appears diffusional (Lin et al., 2018; Goswami et al., 2019). The diffusional behavior arises due to the possibility of moving the charges in either forward or backward direction and therefore differs from delocalized

MOF systems where charges instead move in response to an electric field (Hendon et al., 2012; Talin et al., 2014; Goswami et al., 2018; Park et al., 2018; Xie et al., 2020). If charge diffusion is slow relative to MOF-sited-electrocatalyst activity, diffusion can limit the overall catalytic activity (Hod et al., 2015a; Celis-Salazar et al., 2019; Johnson et al., 2020). Hence, understanding and optimizing the diffusional charge transport within the confined spaces of MOFs is of paramount interest for the development of next-generation heterogeneous electrocatalysts for energy-relevant reactions.

Ruthenium (II) polypyridyl complexes, especially Ru(bpy)₃²⁺ (bpy = 2,2'-bipyridine), have received wide attention in the synthesis of the MOFs (Larsen and Wojtas, 2012; Lin et al., 2017; Choi et al., 2020; Yan et al., 2020; Stanley et al., 2021), both as a linker and as a non-structural ligand, due to their rich photophysical and electrochemical properties. Previously, our group reported the post-synthesis modification of hexazirconium nodes of mesoporous MOF NU-1000 by Ru^{II}(bpy)₂(dcbpy), *i.e.*, bis-(2,2'-bipyridine)-(4,4'-dicarboxy-2,2'-bipyridine) ruthenium(II), and investigated the heterogeneous photocatalytic activity for an oxidative amine-coupling reaction (Nagatomi et al., 2020). Compared to photocatalysis and related photophysics, the electrochemical properties of Ru(bpy)₃²⁺-containing MOFs are relatively less



explored. Morris *et al.* incorporated $\text{Ru}(\text{bpy})_3^{2+}$ within a UiO-67 type framework by mixed ligand approach and then examined the immobilized compound as a light absorber for dye-sensitized solar cells (Maza *et al.*, 2016) and also as an emitter for electro-generated chemiluminescence (Cai *et al.*, 2018). In both cases, charge transport (*i.e.*, transport of redox equivalents) is necessary. For electronically localized species like $\text{Ru}(\text{bpy})_3^{n+}$, charge transport can be achieved by site-to-site redox hopping (and coupled movement of charge-compensating ions) between immobilized complexes. At the microscopic level, redox hopping is equivalent to a series of electron (or hole) self-exchange reactions. At the macroscopic level, redox hopping is diffusive. In this work, we have delineated redox hopping-based charge transport by $\text{Ru}(\text{bpy})_3^{n+}$ sites immobilized in a mesoporous MOF, NU-1008. We have quantified diffusive charge transport within electrode-supported thin films of the functionalized MOF by introducing large or small perturbations of the applied potential *via* chronoamperometry.

RESULTS AND DISCUSSION

Here we have used NU-1008 [$\text{Zr}_6(\mu_3\text{-O})_4(\mu_3\text{-OH})_4(\text{OH})_4(\text{OH}_2)_4(\text{TCPB})_2$] [H_4TCPB = 1,2,4,5-tetrakis(4-(carboxyphenyl)-3,6-dibromo-benzene; TCPB⁴⁻ is a tetratopic linker] as a platform MOF. The [$\text{Zr}_6(\mu_3\text{-O})_4(\mu_3\text{-OH})_4(\text{OH})_4(\text{OH}_2)_4$]⁸⁺ units constitute nodes, and TCPB⁴⁻ ions are linkers (**Scheme 1**) (Lyu *et al.*, 2019). The MOF is of *csq* topology and therefore offers cross-connected triangular and hexagonal 1D channels of $\sim 12 \text{ \AA}$ and 30 \AA diameter, respectively. The cross-connecting pores, *i.e.*, *c*- and *c'*-pores, have a minimum van der Waals width of $\sim 2 \times 7$ and $2.6 \times 10 \text{ \AA}^2$, respectively. Thus, they are significantly narrower than the cross-connecting pores in NU-1000 and PCN-222—closely related MOFs also characterized by *csq* topology. Notably, only the hexagonal channels are wide enough to accommodate $\text{Ru}^{\text{II}}(\text{bpy})_2(\text{dcbpy})$. Similar to what has been observed for NU-1000, non-structural ligands presenting carboxylate, phosphonate, and acetylacetonate functionality can be attached

to the MOF node by displacing labile terminal aqua and hydroxo ligands (bidentate coordination) or only terminal hydroxo ligands (monodentate coordination) (Deria et al., 2014). However, unlike NU-1000 which consists of redox-active tetrakis (4-carboxyphenyl)pyrene linkers (Mondloch et al., 2013; Goswami et al., 2019), TCPB⁴⁻ is redox-inert within the experimental window examined.

Ru^{II}(bpy)₂(dcbpy) was installed in NU-1008 by following a procedure described previously for installation in NU-1000 (Nagatomi et al., 2020). Briefly, pre-synthesized and carefully solvent-evacuated NU-1008 was soaked in an acetonitrile solution of Ru^{II}(bpy)₂(dcbpy) for 24 h at 70°C. Unwanted physisorbed ruthenium species were then removed by vigorously washing the sample with acetonitrile. The porous acetonitrile-filled assembly was then solvent-exchanged with acetone, a low-surface-tension liquid that exerts minimal capillary force and, consequently, has no detectable damage (such as pore collapse) when subsequently removed from the functionalized MOF *via* heating under dynamic vacuum. Ru-bpy@NU-1008 was obtained as an orange powder; NU-1008 is white. Ru^{II}(bpy)₂(dcbpy) installation was confirmed by measuring the ¹H NMR spectrum of the acid-digested sample. By comparing peak integrations for linker *vs.* guest-molecule protons, a loading of ~1 Ru^{II}(bpy)₂(dcbpy) per Zr₆ node was determined, which is similar to the previously reported loading in NU-1000 (Supplementary Figure S1). Additional evidence of the ruthenium complex installation was obtained from ICP-OES analysis, which suggests the loading of 0.83 Ru/Zr₆ node. A loading of one Ru complex per node corresponds to three Ru complexes per hexagon unit, consistent with the loading scheme illustrated above.

Ru-bpy@NU-1008 was sited as a thin film on fluorine-doped tin oxide (FTO) electrode by electrophoretic deposition (EPD; for details, see Supplementary Material) (Hod et al., 2014). Scanning electron microscopy cross-sectional images indicated a film thickness of ~1.3 μm (Figure 1A). When excited at the ¹MLCT band of the Ru^{II}(bpy)₂(dcbpy), a broad emission is expected to be centered at around 650 nm from the ³MLCT excited state (Cai et al., 2018). Figure 1B depicts the emission spectra of a film of Ru-bpy@NU-1008 when excited at 450 and 390 nm.

The electrochemical behavior of thin-film (EPD) versions of the FTO-supported material with and without node-ligated Ru^{II}(bpy)₂(dcbpy) was assessed in a 3-electrode setup in 0.1 M dichloromethane solution of tetrabutylammonium hexafluorophosphate (TBAPF₆), with a Pt wire as a counter-electrode and Ag/AgCl as a reference electrode. Figure 2A presents the cyclic voltammograms for NU-1008 and for Ru-bpy@NU-1008 at various scan rates. Consistent with the redox-inert nature of both the TCPB⁴⁻ linker and the hexa-Zr(IV)-oxy node, no Faradaic current was observed for NU-1008. In contrast, Ru-bpy@NU-1008 shows a chemically reversible oxidation of Ru(II) to Ru(III). From the voltammetry, the Ru(III/II) formal potential is ~1.48 V. Returning to Figure 2A, the intra-film redox process is kinetically sluggish on the various voltammetry timescales as evidenced by scan-rate-dependent differences in anodic *vs.* cathodic peak potentials.

To estimate the D_{hopping} , the apparent diffusion coefficient for redox hopping, chronoamperometry experiments were performed. In these experiments, gradients in concentration of the redox-active species are created by stepping the applied potential from well negative of the formal potential of the immobilized redox couple to well positive (or *vice versa*). Here we stepped the potential from 0 to 2 V and then after equilibration at 2 V back to 0 V. If the time evolution of the resulting Faradaic current is governed by Fick's first and second laws, as applied to 1-D diffusion to a planar surface (the electrode), D_{hopping} can be obtained by fitting the current decay to the Cottrell equation (Eq. 1). In the equation as applied here, n is 1 and is the number of electrons extracted in converting each Ru(II) center to Ru(III), F is the Faraday constant, A is the electrode area, and C is the molar concentration of Ru^{II}(bpy)₂(dcbpy) within the MOF, with the full framework, rather than only the void space, defining the volume for determining C . Here C is ~0.1 M or 1×10^{-4} mol/cm³.

$$i(t) = 2nFACD_{\text{hopping}}^{1/2} / (\pi^{1/2}t^{1/2}) \quad (1)$$

Figure 2B shows the plots of current density (amperes per square centimeter of electrode area) *vs.* $t^{-1/2}$ for oxidation of Ru(II) to Ru(III) and reduction of Ru(III) to Ru(II). From the slopes of the plots at early time, we obtain D_{hopping} values of 6×10^{-12} cm²/s both in the oxidation and reduction direction. For comparison, the D_{hopping} values for linker-based redox hopping in NU-1000 range from 2×10^{-10} to 3×10^{-11} cm²/s in the direction aligned with the MOF channels and $\sim 6 \times 10^{-13}$ cm²/s through the plane that is orthogonal to the channels (Goswami et al., 2019).

Integration of current/time transients from potential step experiments reveals, somewhat surprisingly, that only 1 to 2% of the installed ruthenium centers are electroactive—a finding that is corroborated by the voltammograms in Figure 2A. If the electrophoretically deposited MOF crystallites perfectly and uniformly covered the underlying electrode, leaving no unexposed gaps, and if the deposited crystallites were perfectly oriented with mesoporous channels parallel to the supporting electrode, the observed electroactivity would be equivalent to that from an electroactive zone having a thickness of 5 to 6 mesoporous channels, *i.e.*, ~15–18 nm, with the rest of the film being inactive. If siting and packing of electrophoretically deposited material are less perfect—a distinct possibility given the prolate spheroidal shape (rugby ball shape) of the crystallites—the observed electroactivity could be equivalent to that from an electroactive zone, perhaps two to three times as thick, *i.e.*, *ca.* 30–50 nm.

We speculatively ascribe the unexpected electrochemical inactivity of the majority of the 1,300-nm-thick film to ineffective inter-crystalline charge transport. The oxidation of Ru(II)@NU-1008 sites requires uptake of charge-compensating electrolyte anions (or expulsion intra-channel electrolyte cations). The diameter of PF₆⁻ is ~5.2 Å, while the minimum diameter of the flexible TBA⁺ cation is ~8 Å. Notably, the widths of the channel-interconnecting c and c' pores are less than 3 Å and thus should be blocking toward both PF₆⁻ and TBA⁺. Indeed

electrolyte ion uptake and release should be sterically feasible only at the channel termini. As qualitatively illustrated in **Scheme 1**, the ruthenium-loaded hexagonal mesopores are sterically congested, but the narrower trigonal micropores are not. Thus, we further speculate that charge-compensating electrolyte anions move through the micropores, while the corresponding electrogenerated holes move by hopping between ruthenium sites in the MOF mesopores. Finally, we speculate that, because of the multiplicity of steric constraints for the ingress and egress of charge-compensating ions, the electrochemical communication between MOF crystallites is (1) negligible on timescales relevant to cyclic voltammetry and chronoamperometry and (2) limited, in a practical sense, to only those crystallites of NU-1008 that directly contact the electrode. Spatially resolved assessment of electroactivity should provide a means of assessing the validity of these speculative interpretations. Notably, other *csq* frameworks offering wider *c*-pores (such as NU-1000) and containing smaller redox-functional guests (such as metallocenes) are fully electroactive.

CONCLUSION

In conclusion, solvent-assisted ligand incorporation, in the form of Ru^{II}(bpy)₂(dcbpy) attachment to zirconium-containing MOF nodes, renders the mesoporous Zr-MOF, NU-1008, redox-conductive—a desirable feature for subsequent studies involving framework-isolated electrocatalysts. Ru-bpy@NU-1008 can be electrophoretically deposited on FTO as films of ~1.3- μm thickness and then addressed electrochemically. Cyclic voltammetry yields well-defined signals for the Ru(II/III) couple, with the magnitude of the signals substantially exceeding the signal anticipated for an electrode-contacting monolayer and therefore implying redox hopping between sites proximal to and further from the electrode. Nevertheless, only 1–2% of the installed ruthenium sites are electrochemically addressable. We speculatively ascribe the unresponsiveness of the majority of the installed sites to ion-transport-related steric constraints on inter-crystalline redox communication, such that only those crystallites directly contacting the underlying electrode are electrochemically addressable. From chronoamperometry experiments, the value for D_{hopping} is $6 \times 10^{-12} \text{ cm}^2/\text{s}$. A *ca.* 40-nm-thick electroactive zone can support a catalyst with a TOF of about 2 s^{-1} . Alternatively, if catalysts were sited only at the outer edge of an electroactive zone, greater TOFs could be supported—albeit with a little change in the overall catalytic

REFERENCES

Cai, M., Loague, Q. R., Zhu, J., Lin, S., Usov, P. M., and Morris, A. J. (2018). Ruthenium(II)-polypyridyl Doped Zirconium(IV) Metal-Organic Frameworks for Solid-State Electrochemiluminescence. *Dalton Trans.* 47 (46), 16807–16812. doi:10.1039/c8dt03906b

rate since fewer active sites would be present (Celis-Salazar et al., 2019; Johnson et al., 2020). When combined with the light-harvesting properties of ruthenium complexes, the results suggest that analogues of Ru-bpy@NU-1008 featuring larger-diameter *c*-pores could be usefully functional as sensitizers in photoelectrochemical cells, including photoelectrochemical synthesis cells.

DATA AVAILABILITY STATEMENT

The original contributions presented in the study are included in the article/**Supplementary Material**, further inquiries can be directed to the corresponding author.

AUTHOR CONTRIBUTIONS

JD performed the electrochemical experiments. SG performed the synthesis of the material. JD, SG, and JTH contributed to writing the manuscript.

FUNDING

This work was supported by the US Dept. of Energy, Office of Science, Basic Energy Sciences through grant DE-FG02-87ER13808, and by Northwestern University. This work made use of the Keck-II facility of Northwestern University's NUANCE Center, which has received support from the Soft and Hybrid Nanotechnology Experimental (SHyNE) Resource (NSF ECCS-1542205), and the MRSEC program (NSF DMR1720139) at the Materials Research Center.

ACKNOWLEDGMENTS

We thank Rui Wang for helpful discussions. The authors thank Rebecca Sponenburg and the Northwestern University Quantitative Bioelement Imaging Center (QBIC) for performing ICP-OES measurements.

SUPPLEMENTARY MATERIAL

The Supplementary Material for this article can be found online at: <https://www.frontiersin.org/articles/10.3389/fceng.2021.828266/full#supplementary-material>

Celis-Salazar, P. J., Cai, M., Cucinell, C. A., Ahrenholtz, S. R., Epley, C. C., Usov, P. M., et al. (2019). Independent Quantification of Electron and Ion Diffusion in Metallocene-Doped Metal-Organic Frameworks Thin Films. *J. Am. Chem. Soc.* 141 (30), 11947–11953. doi:10.1021/jacs.9b03609

Chen, Z., Concepcion, J. J., Jurss, J. W., and Meyer, T. J. (2009). Single-Site, Catalytic Water Oxidation on Oxide Surfaces. *J. Am. Chem. Soc.* 131 (43), 15580–15581. doi:10.1021/ja906391w

- Choi, I. H., Yoon, S., Huh, S., Kim, S. J., and Kim, Y. (2020). Photophysical Properties and Heterogeneous Photoredox Catalytic Activities of Ru(bpy) 3 @InBTB Metal-Organic Framework (MOF). *Chem. Eur. J.* 26 (64), 14580–14584. doi:10.1002/chem.202003743
- Deria, P., Bury, W., Hupp, J. T., and Farha, O. K. (2014). Versatile Functionalization of the NU-1000 Platform by Solvent-Assisted Ligand Incorporation. *Chem. Commun.* 50 (16), 1965–1968. doi:10.1039/c3cc48562e
- Ding, B., Solomon, M. B., Leong, C. F., and D'Alessandro, D. M. (2021). Redox-active Ligands: Recent Advances towards Their Incorporation into Coordination Polymers and Metal-Organic Frameworks. *Coord. Chem. Rev.* 439, 213891. doi:10.1016/j.ccr.2021.213891
- Furukawa, H., Cordova, K. E., O'Keeffe, M., and Yaghi, O. M. (2013). The Chemistry and Applications of Metal-Organic Frameworks. *Science* 341 (6149), 1230444. doi:10.1126/science.1230444
- Goswami, S., Hod, I., Duan, J. D., Kung, C.-W., Rimoldi, M., Malliakas, C. D., et al. (2019). Anisotropic Redox Conductivity within a Metal-Organic Framework Material. *J. Am. Chem. Soc.* 141 (44), 17696–17702. doi:10.1021/jacs.9b07658
- Goswami, S., Ray, D., Otake, K.-i., Kung, C.-W., Garibay, S. J., Islamoglu, T., et al. (2018). A Porous, Electrically Conductive Hexa-Zirconium(IV) Metal-Organic Framework. *Chem. Sci.* 9 (19), 4477–4482. doi:10.1039/c8sc00961a
- Hendon, C. H., Tiana, D., and Walsh, A. (2012). Conductive Metal-Organic Frameworks and Networks: Fact or Fantasy? *Phys. Chem. Chem. Phys.* 14 (38), 13120–13132. doi:10.1039/c2cp41099k
- Hod, I., Bury, W., Gardner, D. M., Deria, P., Roznyatovskiy, V., Wasielewski, M. R., et al. (2015). Bias-Switchable Permselectivity and Redox Catalytic Activity of a Ferrocene-Functionalized, Thin-Film Metal-Organic Framework Compound. *J. Phys. Chem. Lett.* 6 (4), 586–591. doi:10.1021/acs.jpcc.5b00019
- Hod, I., Bury, W., Karlin, D. M., Deria, P., Kung, C.-W., Katz, M. J., et al. (2014). Directed Growth of Electroactive Metal-Organic Framework Thin Films Using Electrophoretic Deposition. *Adv. Mater.* 26 (36), 6295–6300. doi:10.1002/adma.201401940
- Hod, I., Sampson, M. D., Deria, P., Kubiak, C. P., Farha, O. K., and Hupp, J. T. (2015). Fe-Porphyrin-Based Metal-Organic Framework Films as High-Surface Concentration, Heterogeneous Catalysts for Electrochemical Reduction of CO₂. *ACS Catal.* 5 (11), 6302–6309. doi:10.1021/acscatal.5b01767
- Islamoglu, T., Goswami, S., Li, Z., Howarth, A. J., Farha, O. K., and Hupp, J. T. (2017). Postsynthetic Tuning of Metal-Organic Frameworks for Targeted Applications. *Acc. Chem. Res.* 50 (4), 805–813. doi:10.1021/acs.accounts.6b00577
- Johnson, B. A., Beiler, A. M., McCarthy, B. D., and Ott, S. (2020). Transport Phenomena: Challenges and Opportunities for Molecular Catalysis in Metal-Organic Frameworks. *J. Am. Chem. Soc.* 142 (28), 11941–11956. doi:10.1021/jacs.0c02899
- Kung, C.-W., Goswami, S., Hod, I., Wang, T. C., Duan, J., Farha, O. K., et al. (2020). Charge Transport in Zirconium-Based Metal-Organic Frameworks. *Acc. Chem. Res.* 53 (6), 1187–1195. doi:10.1021/acs.accounts.0c00106
- Larsen, R. W., and Wojtas, L. (2012). Photophysical Studies of Ru(II)tris(2,2'-bipyridine) Confined within a Zn(II)-Trimesic Acid Polyhedral Metal-Organic Framework. *J. Phys. Chem. A.* 116 (30), 7830–7835. doi:10.1021/jp302979a
- Lei, Z., Xue, Y., Chen, W., Qiu, W., Zhang, Y., Horike, S., et al. (2018). MOFs-Based Heterogeneous Catalysts: New Opportunities for Energy-Related CO₂ Conversion. *Adv. Energy Mater.* 8 (32), 1801587. doi:10.1002/aenm.201801587
- Li, J.-R., Kuppler, R. J., and Zhou, H.-C. (2009). Selective Gas Adsorption and Separation in Metal-Organic Frameworks. *Chem. Soc. Rev.* 38 (5), 1477–1504. doi:10.1039/b802426j
- Lieber, C. M., and Lewis, N. S. (1984). Catalytic Reduction of Carbon Dioxide at Carbon Electrodes Modified with Cobalt Phthalocyanine. *J. Am. Chem. Soc.* 106 (17), 5033–5034. doi:10.1021/ja00329a082
- Lin, S., Pineda-Galvan, Y., Maza, W. A., Epley, C. C., Zhu, J., Kessinger, M. C., et al. (2017). Electrochemical Water Oxidation by a Catalyst-Modified Metal-Organic Framework Thin Film. *ChemSusChem* 10 (3), 514–522. doi:10.1002/cssc.201601181
- Lin, S., Usov, P. M., and Morris, A. J. (2018). The Role of Redox Hopping in Metal-Organic Framework Electrocatalysis. *Chem. Commun.* 54 (51), 6965–6974. doi:10.1039/c8cc01664j
- Lyu, J., Zhang, X., Otake, K.-i., Wang, X., Li, P., Li, Z., et al. (2019). Topology and Porosity Control of Metal-Organic Frameworks through Linker Functionalization. *Chem. Sci.* 10 (4), 1186–1192. doi:10.1039/c8sc04220a
- Majewski, M. B., Peters, A. W., Wasielewski, M. R., Hupp, J. T., and Farha, O. K. (2018). Metal-Organic Frameworks as Platform Materials for Solar Fuels Catalysis. *ACS Energy Lett.* 3 (3), 598–611. doi:10.1021/acsenergylett.8b00010
- Maza, W. A., Haring, A. J., Ahrenholtz, S. R., Epley, C. C., Lin, S. Y., and Morris, A. J. (2016). Ruthenium(II)-polypyridyl Zirconium(IV) Metal-Organic Frameworks as a New Class of Sensitized Solar Cells. *Chem. Sci.* 7 (1), 719–727. doi:10.1039/c5sc01565k
- Mondloch, J. E., Bury, W., Fairen-Jimenez, D., Kwon, S., DeMarco, E. J., Weston, M. H., et al. (2013). Vapor-Phase Metalation by Atomic Layer Deposition in a Metal-Organic Framework. *J. Am. Chem. Soc.* 135 (28), 10294–10297. doi:10.1021/ja4050828
- Nagatomi, H., Gallington, L. C., Goswami, S., Duan, J., Chapman, K. W., Yanai, N., et al. (2020). Regioselective Functionalization of the Mesoporous Metal-Organic Framework, NU-1000, with Photo-Active Tris-(2,2'-bipyridine) Ruthenium(II). *ACS Omega* 5 (46), 30299–30305. doi:10.1021/acsomega.0c04823
- Park, J. G., Aubrey, M. L., Oktawiec, J., Chakarawet, K., Darago, L. E., Grandjean, F., et al. (2018). Charge Delocalization and Bulk Electronic Conductivity in the Mixed-Valence Metal-Organic Framework Fe(1,2,3-triazolate)₂(BF₄)_x. *J. Am. Chem. Soc.* 140 (27), 8526–8534. doi:10.1021/jacs.8b03696
- Stanley, P. M., Haimerl, J., Thomas, C., Urstoeger, A., Schuster, M., Shustova, N. B., et al. (2021). Host-Guest Interactions in a Metal-Organic Framework Isorecticular Series for Molecular Photocatalytic CO₂ Reduction. *Angew. Chem. Int. Ed.* 60 (33), 17854–17860. doi:10.1002/anie.202102729
- Talin, A. A., Centrone, A., Ford, A. C., Foster, M. E., Stavila, V., Haney, P., et al. (2014). Tunable Electrical Conductivity in Metal-Organic Framework Thin-Film Devices. *Science* 343 (6166), 66–69. doi:10.1126/science.1246738
- Xie, L. S., Skorupskii, G., and Dincă, M. (2020). Electrically Conductive Metal-Organic Frameworks. *Chem. Rev.* 120 (16), 8536–8580. doi:10.1021/acs.chemrev.9b00766
- Yan, Y., Li, C., Wu, Y., Gao, J., and Zhang, Q. (2020). From Isolated Ti-Oxo Clusters to Infinite Ti-Oxo Chains and Sheets: Recent Advances in Photoactive Ti-Based MOFs. *J. Mater. Chem. A* 8 (31), 15245–15270. doi:10.1039/d0ta03749d
- Yoshida, T., Tsutsumida, K., Teratani, S., Yasufuku, K., and Kaneko, M. (1993). Electrochemical Reduction of CO₂ in Water by [Re(bpy)(CO)₃Br] and [Re(terpy)(CO)₃Br] Complexes Incorporated into Coated Nafion Membrane (Bpy = 2,2'-bipyridine; Terpy = 2,2',6',6''-terpyridine). *J. Chem. Soc. Chem. Commun.* 7, 631–633. doi:10.1039/c39930000631

Conflict of Interest: The authors declare that the research was conducted in the absence of any commercial or financial relationships that could be construed as a potential conflict of interest.

Publisher's Note: All claims expressed in this article are solely those of the authors and do not necessarily represent those of their affiliated organizations or those of the publisher, the editors, and the reviewers. Any product that may be evaluated in this article or claim that may be made by its manufacturer, is not guaranteed or endorsed by the publisher.

Copyright © 2022 Duan, Goswami and Hupp. This is an open-access article distributed under the terms of the Creative Commons Attribution License (CC BY). The use, distribution or reproduction in other forums is permitted, provided the original author(s) and the copyright owner(s) are credited and that the original publication in this journal is cited, in accordance with accepted academic practice. No use, distribution or reproduction is permitted which does not comply with these terms.